[This is a non-peer-reviewed preprint submitted to EarthArXiv and currently under review in the journal “The Sedimentary Record by SEPM”]

Semi-automated correlation of Silurian well-logs across Gotland, Sweden, using Dynamic Time Warping with Barycenter Averaging

Michiel Arts[1], Daniel Sopher[2], Mikael Calner[3], Mikael Erlström[3], Rohit Samant[4], Bradley Cramer[5]. Anne-Christine Da Silva[1]

1. SediCClim, Geology Department, Liège University, Belgium (michiel.arts@uliege.be)
2. Geological Survey of Sweden, Dragarbrunnsgatan 77, 75319, Uppsala, Sweden
3. Department of Geology, Lund University, Sölvegatan 12, SE-223 62 Lund, Sweden
4. Institute of Geology and Palaeontology, University of Münster, 48149, Münster, Germany
5. Department of Earth and Environmental Sciences, University of Iowa, Iowa City, Iowa, USA

ABSTRACT

Studies of the Silurian sequence on Gotland have significantly advanced our understanding of Silurian climate dynamics, with much of the research focusing on small outcrops and short cores. Gotland has an extensive network of abandoned oil and gas wells. Most of these include gamma-ray well logs, which have not yet been fully utilized for their stratigraphic value. While the Ordovician succession has been successfully correlated using these well logs, the correlation for the Silurian succession has yet to be fully realised. The present study addresses some of the limitations of correlations performed using Dynamical Time Warping (DTW) by combining DTW with Barycenter Averaging (DBA). This enables a semi-automated correlation of the Silurian well-logs over a ~60 km-long transect and the subdivision of gamma-ray log logs into parts that can be linked with their lithostratigraphic surface counterparts. Additionally, we tracked changes in gamma-ray logs associated with these subsurface units, providing new insights into biogeochemical events (e.g., $\delta^{13}C$ excursions) previously mapped only at the surface of Gotland. Our results demonstrate the application of DTW/DBA-based methods for stratigraphic correlation and highlight the potential for integrating subsurface well-log data to refine the Silurian stratigraphy of Gotland.

Keywords: Silurian, gamma-ray well logs, Dynamic Time Warping, subsurface correlation, Barycenter Averaging

INTRODUCTION

The goal of this paper is twofold. Firstly, to introduce a new quasi-automated workflow for well-log correlation, leveraging the DTW algorithm with Barycenter Averaging (DBA). Secondly, to apply and test this approach on a set of gamma-ray well logs from Gotland, Sweden, to improve the well-to-well correlations, thereby enabling a more detailed understanding of the subsurface framework of the Silurian succession beneath Gotland.

Geophysical well logs are an indispensable tool for geoscience, enabling the understanding of subsurface stratigraphy, lithological changes, and depositional facies. Closely spaced well logs enable higher-resolution reconstruction of sedimentary successions than can be achieved with seismic reflection methods. Well-log-based correlations are often performed manually, a time-intensive and subjective process. This limitation highlights the need for automated workflows to analyse large datasets efficiently. Dynamic time warping (DTW) has emerged as a powerful algorithm for this purpose, offering efficient correlation across very different logs, in complex stratigraphic settings (Lineman et al., 1987; Fang et al., 1992; Zoraster et al., 2004; Hladil et al., 2010; Lallier et al., 2012, 2016; Wheeler and Hale, 2014; Wu et al., 2018; Grant et al., 2018; Baville et al., 2022; Sylvester, 2023; Nieminski et al., 2024). By aligning time-equivalent strata across diverse logs, DTW can streamline well-log correlation and improve the resolution of subsurface interpretations.

Three general strategies have emerged for correlating multiple wells using DTW. The first approach propagates stratigraphic surfaces from a single reference well (Wu et al., 2018; Hay et al., 2019). This method depends heavily on the accuracy of the reference curve, as any errors are propagated throughout the correlation network. The second strategy performs pairwise correlations between all wells, followed by a global realignment to ensure consistency (Wheeler and Hale, 2014; Sylvester, 2023; Nieminski et al., 2024). A drawback of this technique is that local mismatches in the pairwise correlations can propagate errors during

the global realignment process, resulting in geologically unrealistic outcomes. This approach can also be computationally intensive, depending on the algorithm used. The third method iteratively refines correlations to converge on a consistent solution (Lallier et al., 2016; Edwards et al., 2018). Although this improves global consistency, it may converge on locally optimal but unrealistic results, particularly without stratigraphic constraints such as biozonations. Like the second approach, it can also be computationally demanding.

To overcome some of the limitations of existing DTW-based methods, we propose a workflow that enhances traditional DTW techniques with two key innovations. This includes the use of relative stratigraphic depth (re)scaling before implementing the DTW algorithm, as well as the creation of an iterative reference curve generation using DTW with Barycenter Averaging (DBA). The iterative approach enables the reference curve to evolve dynamically based on the ensemble of input well logs, thereby reducing the bias that would be present if one relied on a single reference log.

The workflow is applied to a dataset of gamma-ray well logs from Gotland, Sweden. The island has long been recognised for its Silurian succession, including major biogeochemical events such as the Ireviken, Mulde, Linde, and Lau events (Jeppsson, 1996; Jeppsson and Calner, 2002; Calner et al., 2004a, 2004b; Calner and Eriksson, 2006a; Eriksson and Calner, 2008; Vandenbroucke et al., 2013; Biebesheimer et al., 2021; Hartke et al., 2021; Erlström et al., 2022). Although outcrops and shallow cores from Gotland have yielded valuable insights into Silurian climate and biosphere dynamics, their stratigraphic thickness is often limited. Indeed, among the Silurian biogeochemical events, only the formations encompassing the Lau Event have been extensively mapped in the shallow subsurface using well logs (Eriksson and Calner, 2008; Erlström et al., 2022).

Two of the key wells in this study are the Altajme core and the St. Sutarve 2018 well, available in their original high-resolution digital form, unlike the rest of the dataset, which consists of digitized records. The Altajme core/well offers one of the highest-resolution $\delta^{13}C_{carb}$ records of the Silurian (Biebesheimer et al., 2021; Hartke et al., 2021; Stolfus et al., 2023), encompassing

both the Ireviken and Mulde events. Integrating this core with gamma ray logs from Gotland enables a regional contextualization. The St. Sutarve-2018 well is central in the geological framework of the subsurface of Southern Gotland (Erlström et al., 2022). Placing this well within a broader regional context will enable a more refined understanding of the geological evolution of Gotland. The implemented workflow will improve stratigraphic correlations across a transect of approximately ~60 kilometres, linking surface and subsurface data, but also establishes a new avenue for the application of Dynamic Time Warping in stratigraphic studies.

GEOLOGICAL SETTING

The Silurian succession on Gotland was deposited in the Baltic Basin, an intracratonic basin on the palaeocontinent Baltica. During the Silurian, Gotland was located on the northwest flank of the basin, where the water depth increased to the southeast (Baarli et al., 2003). The thickness of the succession increased from circa 250 m in the north to circa 500 m in the south of Gotland, as the basin has a gentle dip of 0.2-0.4 degrees to the southeast. Baltica was located ~10-20° south of the equator during the Silurian, and deposition occurred in a tropical to subtropical setting. The succession is typified by approximately 100 carbonate platforms that prograded from the northeast to southwest during the Silurian (Bjerkéus and Eriksson, 2001; Flodén et al., 2001; Tuuling and Flodén, 2013). These platforms fingers out into in deeper marine depositional settings to the S-SE. The resulting stratigraphy consists of alternating shale or marl and reefal limestone, forming a south-eastward-prograding sequence (Jeppsson, 1996; Calner et al., 2004b, 2004a; Calner, 2005; Calner and Eriksson, 2006a; Jeppsson et al., 2006). Due to erosion and the regional dip, progressively younger strata are exposed toward the southeast.

Within individual units, shallow-water facies such as reefal carbonates dominate the northwest, transitioning to deeper-water shales and marls in the southeast. A long-term shallowing trend during the Silurian led to the gradual south-eastward progradation of reefal facies, with shallow reef deposits reaching southeastern Gotland by the Ludfordian (Bjerkéus and Eriksson, 2001; Flodén et al., 2001; Tuuling and Flodén, 2009).

The Silurian strata of Gotland, Sweden, provide an exceptional record of biotic, geochemical, and lithological changes during the Silurian, including the Ireviken, the Mulde, Linde and Lau events (Aldridge et al., 1993; Jeppsson et al., 2006, 1995; Jeppsson and Aldridge, 2000; Calner et al., 2004a, 2004b; Calner and Eriksson, 2006b; Vandenbroucke et al., 2013; Younes et al., 2017; Bowman et al., 2019; Biebesheimer et al., 2021; Hartke et al., 2021; Stolfus et al., 2023; Claussen, 2024). These events represent major perturbations to the Earth's climate system, characterised by extinction episodes, shifts in carbon isotope signatures, and substantial changes in marine ecosystems and depositional environments.

The Ireviken Event is the oldest Silurian event recorded on Gotland and spans the Llandovery-Wenlock boundary interval, and is represented in the Lower Visby to Hangvar. The Ireviken Event is associated with a major extinction event and a positive $\delta^{13}C$ excursion (Jeppsson, 1987; Melchin et al., 2005, 2020; Cramer et al., 2010; Rose et al., 2019). The Mulde Event, occurring during the Homerian Stage (~428 Ma), is preserved in the Fröjel to Klinteberg formations and linked to a minor extinction and a positive $\delta^{13}C$ excursion (Samtleben et al., 2000; Calner and Jeppsson, 2003; Calner et al., 2006; Jeppsson et al., 2006). The Linde Event took place in the early Ludfordian and is associated with a minor extinction and a tiny $\delta^{13}C$ excursion (Jeppsson and Aldridge, 2000; Claussen, 2024). The Lau Event took place in the late Ludfordian and is associated with a major extinction event and one of the largest $\delta^{13}C$ excursions of the entire Phanerozoic (Calner and Eriksson, 2006a; Calner, 2008; Eriksson and Calner, 2008; Younes et al., 2017; Frýda et al., 2021). The Lau Event is recorded in the Botvide member of the När Formation and the Eke and Burgsvik formations (Jeppsson, 1998; Calner, 2005; Eriksson and Calner, 2008; Erlström et al., 2022).

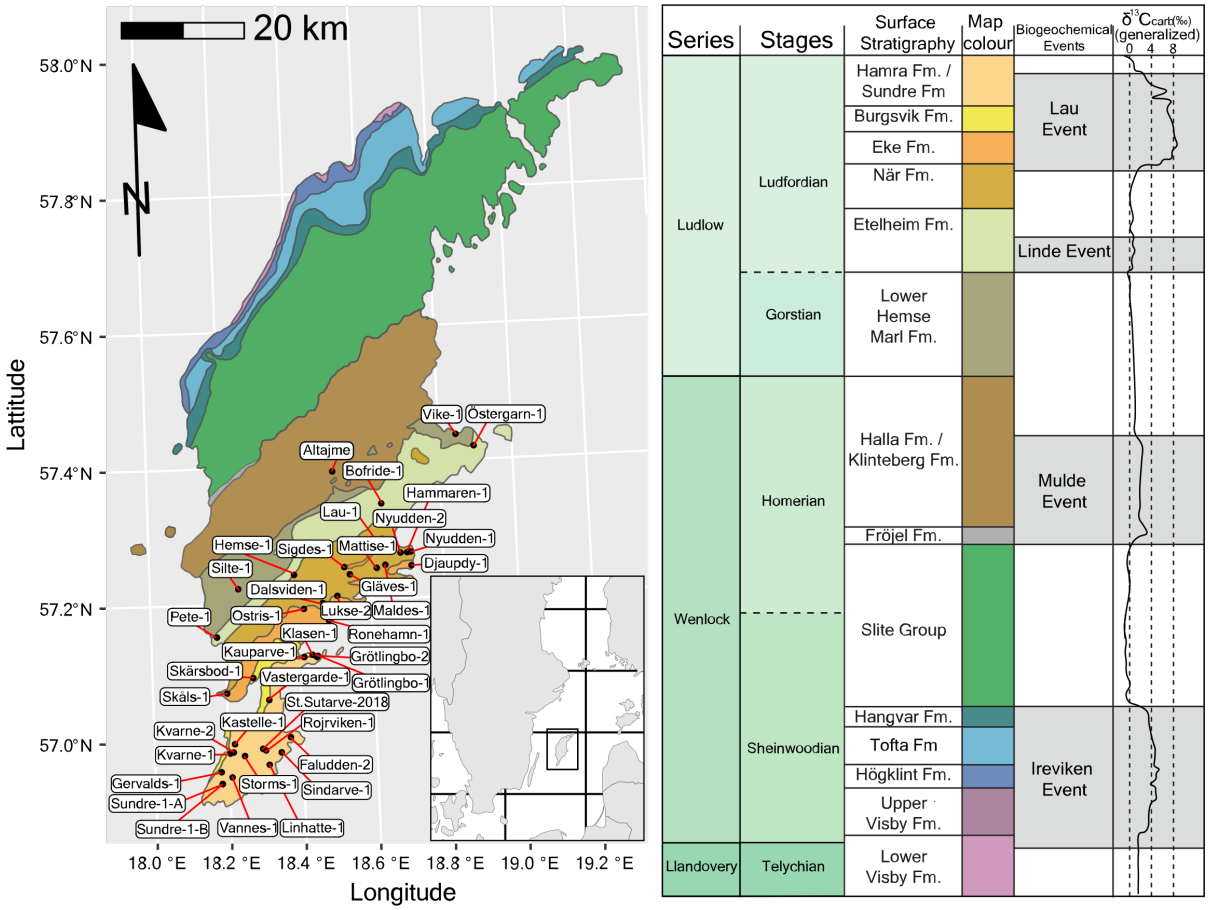

Figure 1. Location of the wells used in this study and the stratigraphic column of the surface succession of Gotland. The Geological map of Gotland (modified after Manten, (1971) and Calner et al. (2004a)). The locations of the forty wells included in this study are marked as black dots. The lithological column/legend and event stratigraphy and $\delta^{13}C_{carb}$ curve is based on Calner, (1999), Jeppsson and Aldridge (2000), Calner and Jeppsson (2003) and Calner et al. (2004a).

MATERIALS AND METHODS

This study utilizes a total of thirty-eight gamma-ray well logs from Gotland (see Figure 1 and SI.1), several of which have been published (Sopher et al., 2016; Erlström and Sopher, 2019; Levendal et al., 2019; Erlström et al., 2022). The Altajme and St. Sutarve 2018 wells are available in original high-resolution digital form, while the rest belong to the legacy OPAB dataset managed by the Swedish Geological Survey (SGU). Originally acquired as analog paper logs by Oljeprospektering AB (OPAB) between 1960 and 1990, a subset of these has

since been digitized by SGU. Missing or incomplete logs were manually digitized for this study using the Log-Evolve™ software (see SI.1).

The wells sampled in this study represent more distal shelfal successions rather than shallow reefal carbonates (see Figure 1 and geological setting), making them especially suitable for dynamic time warping (DTW) since they offer greater continuity and completeness. To compare surface geology with subsurface gamma ray records, surface maps from Manten (1971) and Calner et al. (2004a) were digitized in QGIS and integrated with literature data.

Gamma ray logs, the primary data type used, reflect natural radiation from Potassium-40, Uranium-238, and Thorium-232 in surrounding rocks (Ellis and Singer, 2007). Since spectral gamma data are unavailable for Gotland, interpretations focus on relative changes in log motifs. The logs have a vertical resolution of about 0.15 to 0.3 meters (Ellis and Singer, 2007). The limited resolution, combined with the inclusion of legacy data, restricts the ability to correlate on a bed-by-bed basis. As such, we will focus on general patterns, inflexion points, and prominent metre-scale peaks and troughs.

All gamma-ray logs were normalized to a scale of -1 to 1 for consistent cross-well comparison. Logs were aligned and stretched to a common depth scale, a technique often referred to as placing data in "relative geological time" (Sylvester, 2023). DTW-based studies typically apply this concept as a means to close loops and correct errors after DTW correlations have been conducted (De Bruin et al., 2007; Lomask et al., 2009; Qayyum et al., 2015; Wu et al., 2022; Sylvester, 2023).

Pre-stretching offers a clear advantage since DTW compares patterns within time-series data, and without accounting for thickness variations, stratigraphically equivalent features may misalign. The pre-stretching was guided by six manually selected tie points corresponding to key stratigraphic features (see Figure 2). The well logs were stretched to the average observed thickness between two tie-points in the set of wells. Logs were stretched to the average thickness observed between tie points. The Altajme and Vike-1 wells were excluded from the

191 average thickness calculation since the upper intervals of these wells are impacted by a
192 prograding reefal system during the Mulde Event (Biebesheimer et al., 2021).

193 Tie point set (1) marks a positive gamma-ray inflection corresponding to the base of the
194 Silurian (Sopher et al., 2016; Erlström and Sopher, 2019; Erlström et al., 2022). Set (2) aligns
195 with a negative inflection linked to the S2-S3 sequence boundary in the Baltic Basin and
196 roughly coincides with the onset of the Ireviken Event (see Figure 2) (Lazauskiene et al., 2003;
197 Hartke et al., 2021; Erlström et al., 2022). Set (3) corresponds to a gamma-ray trough at the
198 base of the Mulde Event (see Figure 2 and SI.2.) (Calner et al., 2006; Erlström et al., 2022).
199 Despite differing log expressions, this tie point could be identified in both the Altajme and
200 Grötlingbo-1 wells, aided by the presence of the Mulde $\delta^{13}C_{carb}$ excursion in both records (see
201 SI.2) (Calner et al., 2006). Set (4) is a positive gamma-ray inflexion that marks the approximate
202 termination of the Mulde Event, which again could be identified with the help of the records
203 from the Altajme and the more distal Grötlingbo-1 wells/cores. Set (5) is a minor gamma-ray
204 peak traceable across most wells (see Figure 2). Set (6) is a negative inflexion in the
205 gamma-ray log, which marks the boundary between the Hemse Group and Eke Formation
206 (Eriksson and Calner, 2008; Erlström et al., 2022).

207 Due to the regional dip and erosion, increasingly thicker intervals of younger Silurian strata
208 are missing toward the northwest of Gotland (see Geological setting). As a result, one or more
209 stratigraphic tie-points may be absent in that direction. The missing tie points prevent
210 stretching to a common depth scale. In such cases, missing intervals were filled using a
211 median curve derived from the complete well logs.

212 Once the tie points were defined and the data were pre-stretched, we applied the correlation
213 algorithm. DTW aligns one well log with another (a pairwise technique) without considering
214 the broader stratigraphic context. This often produces inconsistent correlations when extended
215 across multiple wells, also known as the DTW open-loop problem (Sylvester, 2023). To
216 address this, we used Dynamical Time Warping with Barycenter Averaging (DBA), which
217 iteratively averages aligned logs to generate a regional reference gamma-ray curve that

reflects the major correlateable lithological features across all wells (Petitjean et al., 2011; Sardá-Espinosa, 2019).

The DBA process can introduce blocky or spiky artefacts due to its tendency to over-sample flat regions. These artefacts were removed using a Taner bandpass filter, followed by a LOWESS regression to preserve local extremes while removing broader trends. From the resulting smoothed and detrended reference curve, the hundred and fifty largest amplitude peaks were identified as regional correlation points. The DTW algorithm was then applied between the reference curve and each of the thirty-eight original well logs, allowing these regional tie-points to be transposed onto individual logs. These tie points serve as the basis for drawing correlation lines across all wells, supporting detailed subsurface interpretation.

The full R script implementing this workflow is provided in SI.3. It uses the DBA function from the dtwclust package for Barycenter Averaging (Sardá-Espinosa, 2019), the dtw function from the dtw package for time-series alignment (Giorgino, 2009), and several functions from the astrochron package for intermediate processing (Meyers, 2019). Together, these tools enable a semi-automated and reproducible approach for basin-scale well-log correlations.

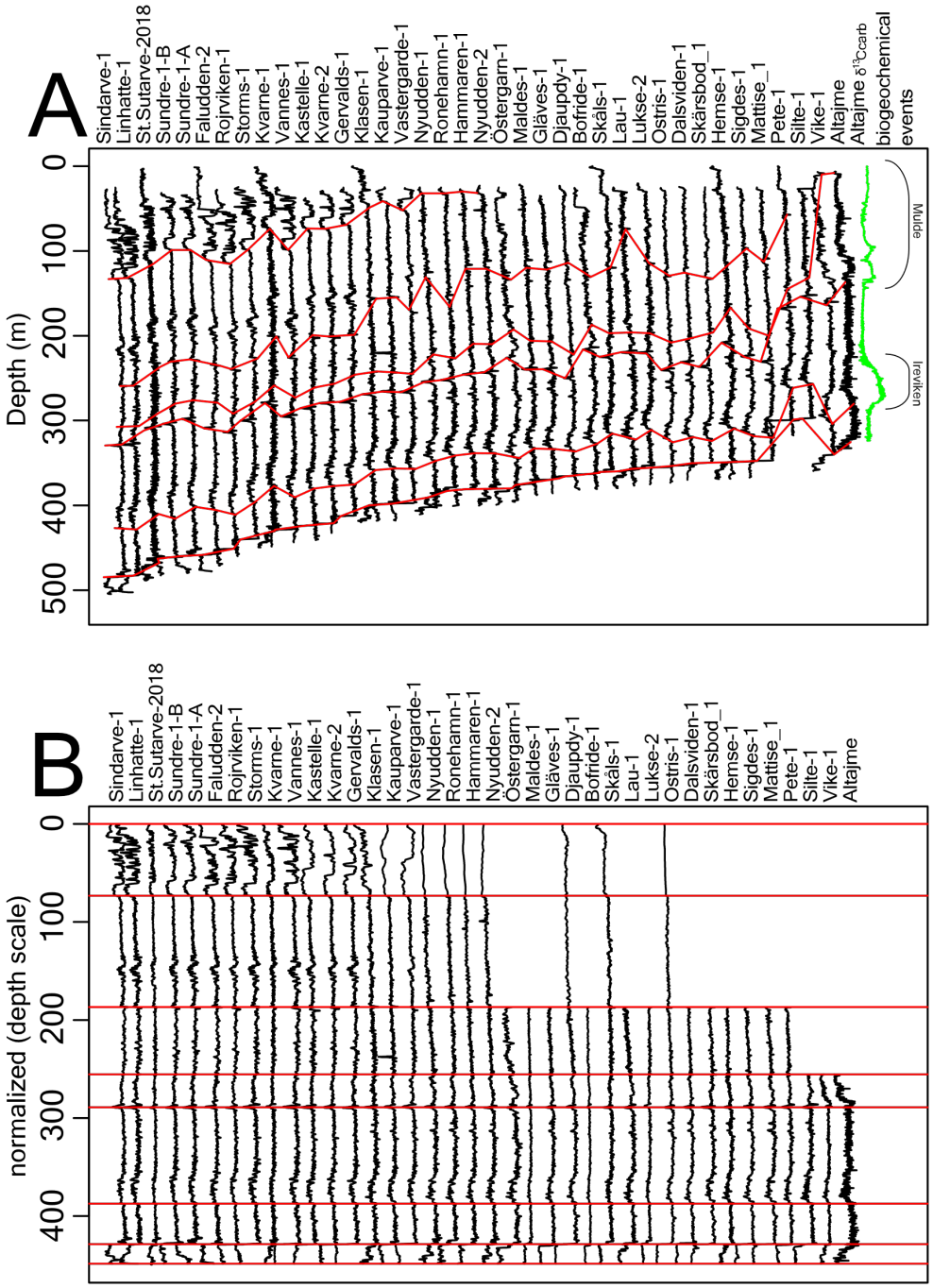

233

234 **Figure 2. The well-logs pre and post stretching . A.** The thirty-eight gamma-ray well logs, with
235 the original manual tie points and correlation lines (red lines). Included is the $\delta^{13}C_{carb}$ curve of
236 the Altajme core and Silurian biogeochemical events identified in this record (Biebesheimer et
237 al., 2021; Hartke et al., 2021). **B.** All the gamma-ray logs stretched between the tie-points to
238 a common depth scale. Note that the normalised logs, plotted side by side, are sorted in order
239 of depth to the base of the Silurian.

RESULTS

The DBA algorithm produced a regional gamma-ray reference curve based on the thirty-eight gamma-ray logs (Figure 3A), which was then denoised and detrended (Figures 3A and B). From the detrended curve, a hundred and fifty data points with the largest deviations from the mean trendline were identified as key tie-points for basin-scale correlation (Figures 3B and C).

Each of the thirty-eight gamma-ray logs was aligned to the reference curve using DTW, enabling the hundred and fifty tie-points to be transposed into individual well logs (see Figure 4). This allowed for the automatic generation of correlation lines between corresponding tie-points (Figure 4A and B). It also allowed the construction of a cross-section along a ~60 km transect from the Sindarve-1 well to the Altajme core/well (Figure 4B). The correlated transect spans depositional settings from shallowest reefal (Altajme) to the deepest marine environment (Sindarve-1), offering a detailed view of lateral stratigraphic variations within the Silurian succession of Gotland.

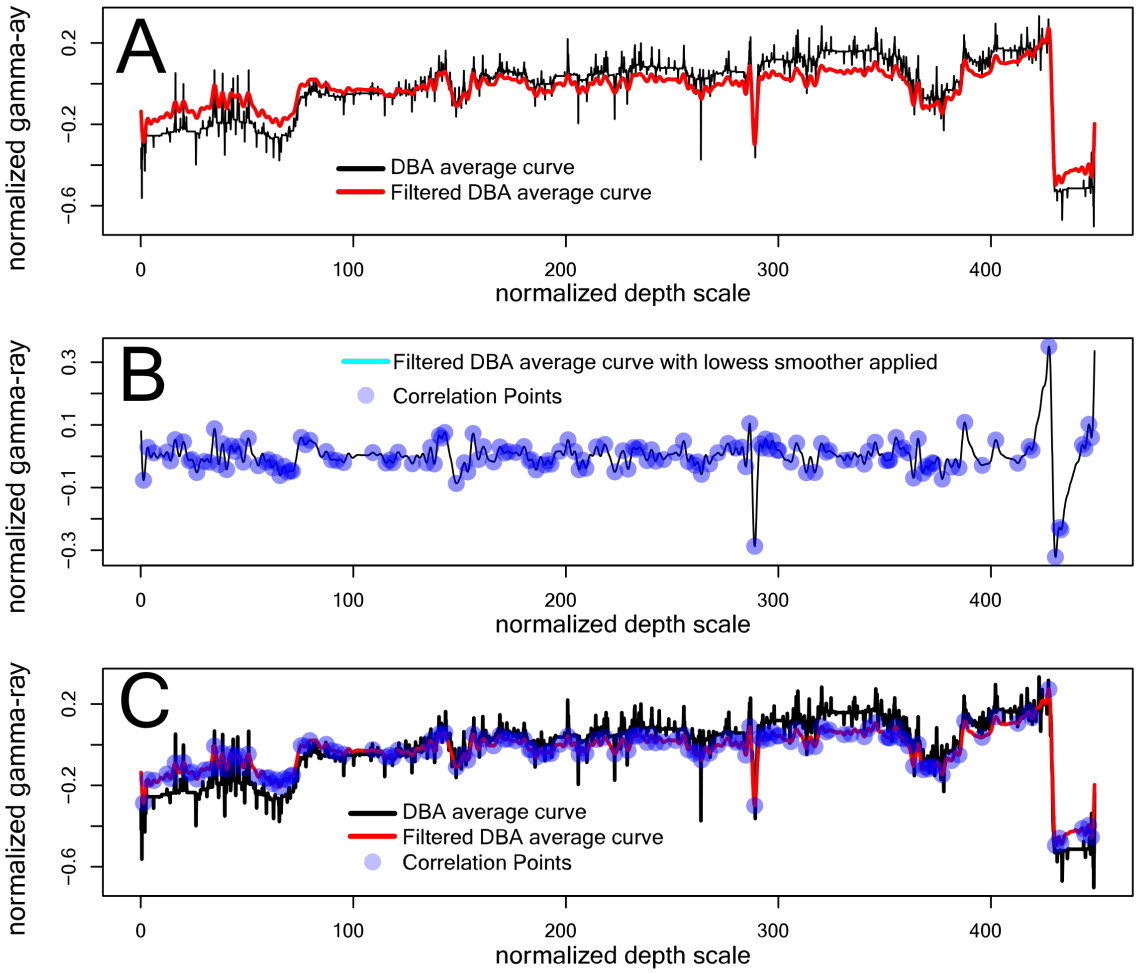

254

255 **Figure 3. The reference curve and its derived correlation points. A.** DBA average curve
256 (black line) and the denoised curve (red line), **B.** Detrended and denoised DBA average curve
257 (light blue line) and the hundred and fifty correlation points (purple points), **C.** DBA average
258 curve (black line), the denoised curve (red line) and the hundred correlation points (purple
259 points).

260

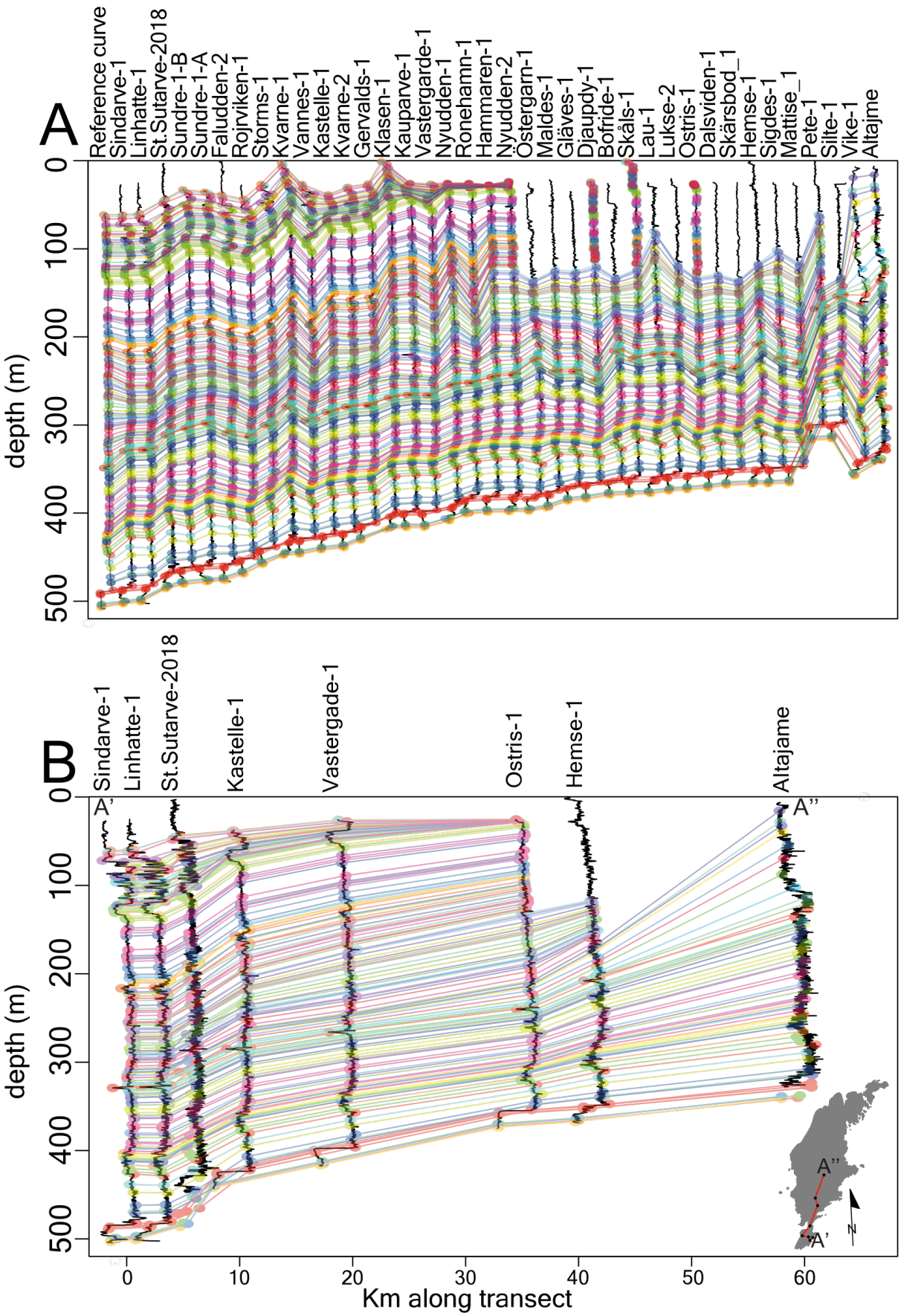
A
Reference curve
Sindarve-1
Linhatte-1
St.Sutarve-2018
Sundre-1-B
Sundre-1-A
Faludden-2
Rojrviken-1
Storms-1
Kvarne-1
Vannes-1
Kastelle-1
Kvarne-2
Gervalds-1
Klasen-1
Kauparve-1
Vastergarde-1
Nyudden-1
Ronehamn-1
Hammaren-1
Nyudden-2
Östergarn-1
Maldes-1
Gläves-1
Djaupdy-1
Bofride-1
Skåls-1
Lau-1
Lukse-2
Ostris-1
Dalsviden-1
Skärsbod_1
Hemse-1
Sigdes-1
Mattise_1
Pete-1
Silte-1
Vike-1
Altajme
depth (m)
0
100
200
300
400
500
B
Sindarve-1
Linhatte-1
St.Sutarve-2018
Kastelle-1
Vastergade-1
Ostris-1
Hemse-1
Altajame
A'
A''
depth (m)
0
100
200
300
400
500
0
10
20
30
40
50
60
Km along transect
A''
A'
N

261

Figure 4. correlation lines drawn between the correlation points. A. All of the thirty-eight gamma-ray logs with the DBA-derived correlation points and lines. Note that we show the normalised logs, plotted side by side, sorted in order of the depth to the base of the Silurian. The reference well was shifted down by 60 metres. B. The well-logs along the A'-A'' transect and their DBA-derived correlation points and lines. The X-axis is kilometres along the transect. The normalized logs are plotted with the same amplitude scale, while maintaining their distance along the profile. For the location of the A'-A'' transect, see the regional map in the bottom right-hand corner

DISCUSSION

On the use of the DBA-based workflow for well-log correlations

This study introduces a comprehensive and reproducible workflow for DTW/DBA-based well-log correlation, implemented in the R programming language (see S.I.3). It advances existing DTW based approaches through two key innovations: (1), the incorporation of relative stratigraphic depth (re)scaling before DTW alignment, and (2) the iterative construction of a reference curve using Dynamic Time Warping with Barycenter Averaging (DBA).

The (re)scaling step integrates geological expertise directly into the model. It ensures that stratigraphic features that are expected to align do so, even when they appear stretched or compressed across different well logs. This pre-alignment improves correlation accuracy and geological coherence. A drawback of this step is that a certain amount of manual work is required to pick the tie points. This makes the process slower and introduces some subjective elements to the process.

Using the DBA algorithm addresses a key limitation of relying solely on DTW. When DTW is used to track lines through a network of wells, the lines often diverge and misalign when traced back to the starting well (Sylvester, 2023). A common workaround involves correlating all wells to a single reference log (Wu et al., 2018; Hay et al., 2019), but this approach will propagate any inaccuracies that are present in the reference curve. The DBA algorithm generates a regional reference curve by iteratively averaging multiple well logs. This reduces the influence

of local anomalies and produces a more reliable and geologically representative reference curve for the correlation framework.

The successful generation of a regional reference curve using the DBA algorithm was made possible by the relatively high degree of similarity among the well logs, which reflects the basin's “layer cake” stratigraphy. Nonetheless, careful pre-processing was essential, given the range of depositional environments represented in the dataset, from lagoonal and reefal facies to deeper basinal settings (Samtleben et al., 2000; Jorgensen et al., 2018; Biebesheimer et al., 2021; Hartke et al., 2021; Erlström et al., 2022). Pre-processing steps included the introduction of tie-points to pre-stretch the data to a common depth scale and padding missing intervals with an average curve where necessary. This highlights the importance of integrating independent stratigraphic information, including biostratigraphy, carbon isotopes, or existing stratigraphic (core) studies, to guide the DBA in producing a representative reference curve of the regional stratigraphy.

Although effective in uniform stratigraphic settings, the use of a regional reference curve has limitations. Other DTW-based methods may be more appropriate in basins with significant lateral variability, such as those with meander belts, large prograding clinoforms, or turbidite deposits (Sylvester, 2023; Nieminski et al., 2024).

The correlation lines in this study show strong geological coherence, but some imperfections remain. For example, the upper bundle of correlation lines between 0 and 140 m in the Sindarve-1 well converges into a single point at the Ostris-1 well (see Figure 4). The convergence of correlation lines does not accurately reflect the geology of Gotland, which has a dip of (0.2-0.4) degrees towards the South (East), so near-surface correlation lines should end at the surface (Dahlqvist and Triumf; Erlström et al., 2022).

In summary, the pre-stretching and DBA-based reference curve workflow provides a fast, effective way to generate numerous geologically sound correlation lines across a basin. However, these results should always be judged against existing knowledge and, where needed, corrected to ensure an accurate interpretation of the basin’s stratigraphy.

Subsurface stratigraphy and correlations in Gotland

The DBA-derived correlation lines enabled the subdivision of Gotland's subsurface succession into fifteen units (see Figure 5), further refining the ten subdivisions previously proposed by Erlström et al. (2022) for Gotland's subsurface. The fifteen intervals are correlated to previously established surface and shallow subsurface units on Gotland (Calner et al., 2004a; Calner and Eriksson, 2006a; Eriksson and Calner, 2008; Biebesheimer et al., 2021; Hartke et al., 2021; Erlström et al., 2022; Stolfus et al., 2023). Unit names reference surface equivalent formations for convenience but do not imply formal naming or redefinition of the subsurface stratigraphy. Some uncertainty remains, especially for deeper units like the Fröjel Formation and older ones, which lack explicit surface correlations in the studied boreholes. Consequently, the stratigraphic naming convention used in this study should be viewed as tentative.

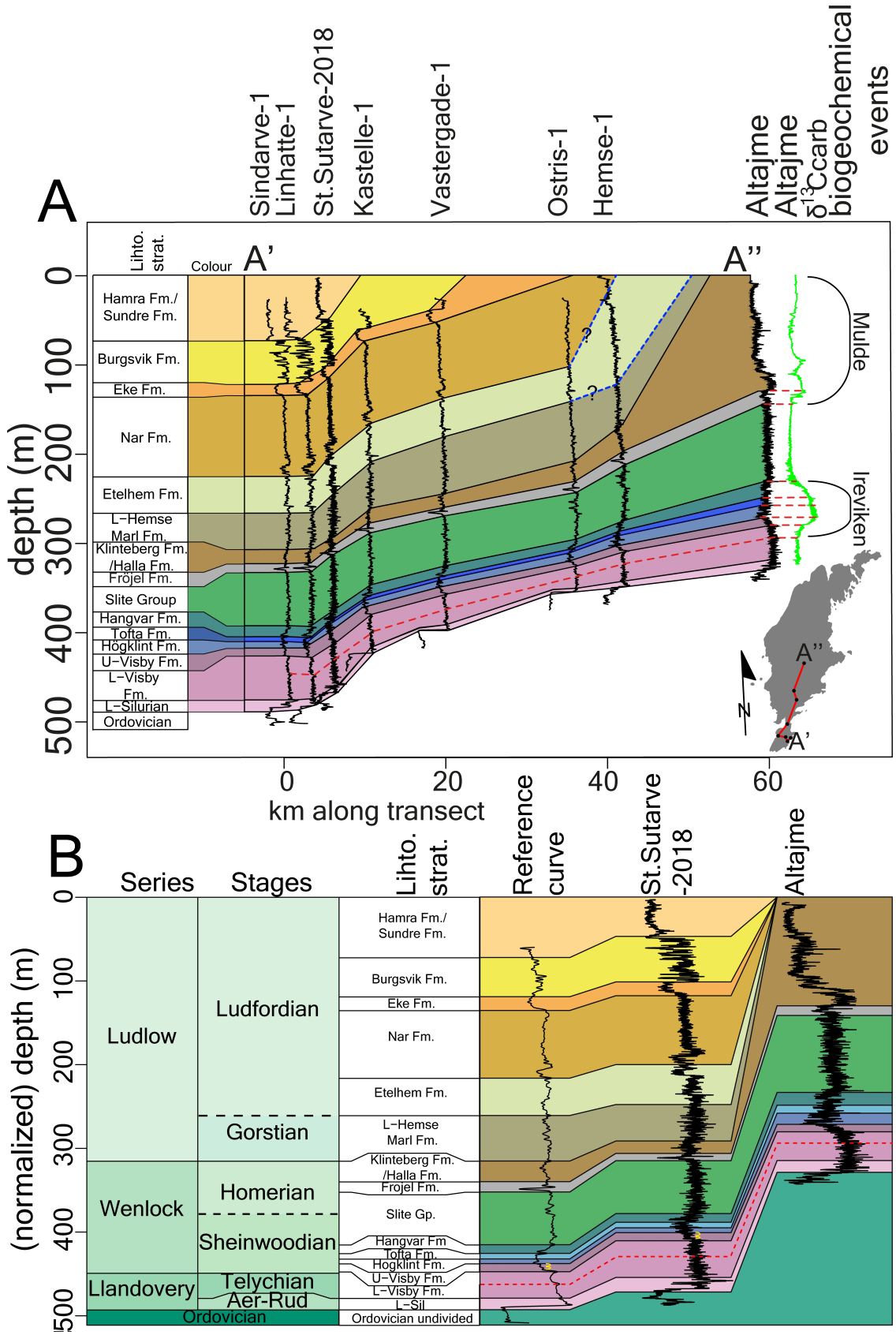

328

329 **Figure 5. Gotland's subsurface succession and its correlation . A.** Correlation of units along

330 the transect A'-A''. The normalised logs are plotted with the same amplitude scale at the

331

corresponding distance along the profile. The location of the transect is shown in the bottom right of the figure. For the locations of wells, see figure 1. The terminations of the boundaries are based on the geological maps of Gotland (Manten, 1971; Calner et al., 2004a). Grey dotted lines with question marks indicate uncertainty in the location of the boundaries of the different units. The red dotted line marks the correlation of a small gamma-ray peak, indicating the onset of a minor rise in the $\delta^{13}C_{carb}$ curve, associated with the Ireviken Event. **B.** Stratigraphic units and the well-log as expressed in the reference curve (generated by the DBA algorithm as part of the correlation process), St.Sutarve-2018, and Altajme wells. The black dotted horizontal lines indicate stage boundaries where their actual locations remain uncertain. The red dotted line marks the correlation of a small gamma-ray peak, indicating the onset of a minor rise in the $\delta^{13}C_{carb}$ curve, associated with the Ireviken Event. The yellow half-circles mark the two peaks that are superimposed upon the declining trend in the gamma-ray log of the Upper Visby Formation.

The stratigraphically lowest and oldest Silurian unit identified in this study is not exposed at the surface. This unit has until now only been identified in the Grötlingbo-1 well/core, where it was identified based on an integrated biostratigraphic study, which indicates the presence of a Rhuddanian to Aeronian-aged unit, separated by a gap spanning the late Aeronian to early Telychian (Männik et al., 2015). The lower Silurian unit is typified by higher gamma-ray values than the overlying Lower Visby Formation. A sharp rise in gamma-ray intensity marks the base of the lower Silurian unit. Variations in thickness and gamma-ray response within this unit create uncertainty about consistently assigning it to a specific stage or biostratigraphic interval across the study area. Further research is needed to clarify its stratigraphic affinity.

The base of the Lower Visby Formation coincides with a transition from the high gamma-ray values of the lower Silurian unit to the stable and moderately high gamma-ray values of the Lower Visby Formation. The top of the Lower Visby is marked by a peak in the gamma-ray log. This peak is preceded by a smaller peak in the gamma-ray log, which marks the onset of a minor rise in the $\delta^{13}C_{carb}$ curve, associated with the Ireviken Event (see Figure 5A). The

smaller gamma-ray peak likely represents the onset of a period of enhanced primary productivity before the Ireviken Extinction Event (Vandenbroucke et al., 2013; Hartke et al., 2021; Stolfus et al., 2023). The smaller gamma-ray peak below the Lower to Upper Visby formational boundary can be easily tracked across the different well logs, confirming the utility of this peak in the stratigraphic correlation. The base of the Lower Visby Formation coincides with a transition from the high gamma-ray values of the lower Silurian unit to the stable and moderately high gamma-ray values of the Lower Visby Formation.

The Upper Visby Formation corresponds to an interval of rising $\delta^{13}C_{carb}$ values and a steady decrease in gamma-ray log values (Figure 5). In the well logs spanning the transect between the Sindarve-1 and Vastergade-1 wells, two small but noticeable peaks can be observed, which are superimposed upon the declining trend in the gamma-ray log of the Upper Visby Formation (see Figure 5). These two peaks are absent in the shallower part of the basin that spans the Ostris-1, Hemse-1, and Altajme wells. The absence of these peaks suggests that part of the Upper Visby Formation is missing in the shallower parts of the basin, which is consistent with the unconformable nature observed for some of the boundaries between the Upper Visby Formation and the Högklint Formation (Manten, 1971; Jeppsson et al., 2006; Cramer, 2009). The variable gamma-ray response of this boundary necessitated the manual tracking of this formational boundary, highlighting a limitation in the process that generated the DTW-based correlation lines.

The Högklint Formation is characterized by low gamma-ray values, exhibiting a gradually increasing trend. In the Altajme Core, this unit is typified by numerous small, positive δ^{13}Ccarb peaks (~1‰) that are superimposed on the larger peak. Sadly, the gamma-ray log lacks the resolution to resolve these finer-scale geochemical features. A distinct positive inflexion in the gamma-ray log marks the boundary with the overlying Tofta Formation. Stable, high $\delta^{13}C_{carb}$ values and low gamma-ray values typify the Tofta Formation. A positive gamma-ray inflexion marks its upper boundary with the Hangvar Formation.

The Hangvar Formation is characterized by numerous small negative δ¹³Ccarb peaks (~1‰) that are superimposed on a larger declining trend (Hartke et al., 2021). Unfortunately, the gamma-ray log lacks the resolution to describe the relationship between the log and these small δ¹³Ccarb peaks. In the Hangvar Formation, the gamma-ray values first show a drop, followed by a gradual upward trend. The transition to the Slite Group is marked by an evolution towards more stable baseline gamma-ray values.

The Slite Group is characterised by consistently high gamma-ray values, lacking internal features suitable for further subdivision. A sharp negative inflexion in the gamma-ray log characterizes its boundary with the overlying Fröjel Formation.

The Fröjel Formation exhibits a distinct gamma-ray trough followed by a sharp positive inflexion at its upper boundary, which coincides with a rise in $\delta^{13}C_{carb}$ values and the extinction interval of the Mulde Event (Hartke et al., 2021; Stolfus et al., 2023).

The Halla/Klinteberg formations are characterized by intermediate gamma-ray values forming a broad trough between the lower values of the Fröjel Formation and the higher values of the Slite Group. The Halla/Klinteberg formations lack clear internal markers, which prevents a subdivision on a formational level. The Halla/Klinteberg formations correspond to the double $\delta^{13}C_{carb}$ peak of the Mulde Event (Calner et al., 2004a; Radzevičius et al., 2014; Biebesheimer et al., 2021). The notably greater thickness of the Halla/Klinteberg formations in the Altajme and Vike-1 wells, compared to more southerly locations, reflects enhanced reef development during the Mulde Event (Samtleben et al., 2000; McLaughlin et al., 2019; Biebesheimer et al., 2021). The significant difference between the Altajme well/core and other records hinders the correlation of the $\delta^{13}C_{carb}$ peaks into the distal part of the basin. High-resolution $\delta^{13}C_{carb}$ profiles are therefore needed for a better understanding of the relationship between gamma-ray log patterns and the carbon-isotope signal. Moreover, reefal influence in the Altajme core has altered the gamma-ray expression of the Halla/Klinteberg and possibly the Fröjel formations, making it unrepresentative of the more distal southern wells. Within the broader correlation framework, the gamma-ray motif of the St. Sutarve-2018 well is considered more

representative for characterizing the Halla/Klinteberg, Fröjel, and younger formations (see Figure 5).

A positive inflection in the gamma-ray log values defines the boundary between the Klinteberg and the Hemse formations. On the surface, the boundary between the Klinteberg and the Hemse formations is defined by the lithological transition from reefal carbonates to marls. This transition is interpreted as diachronous, depending on the local depositional setting (Flodén et al., 2001; Calner and Jeppsson, 2003; Calner et al., 2004a). In the subsurface, the thickness and well-log records of the underlying Halla/Klinteberg Formation do not change much in the transect between the Hemse-1 and Sindarve-1 wells, nor does the gamma-ray signature of the boundary itself change much (see Figure 5).

The Lower Hemse Marl Formation is marked by high and consistent gamma-ray values, with an increased variability at the boundary with the overlying formation (Etelhem formation). The shallower well-logs display an invariant gamma-ray log response (see Figures 4 and 5).

The Etelhem Formation is typified by high gamma-ray values, punctuated by irregular peaks and drops in the gamma-ray log. Surface studies associate the Linde Event with the lower part of the However, the absence of biostratigraphic and geochemical proxy data for this interval in the subsurface limits the ability to identify the Linde Event confidently.

A significant gamma-ray drop marks the base of the När Formation, potentially corresponding to the Millklint limestone unit (Calner et al., 2004a; Jeppsson et al., 2006), though its exact stratigraphic position remains uncertain. The När Formation is generally characterized by stable gamma-ray values, aside from a distinct trough at its base. The Lau Event begins within the Botvide Member of the När Formation (Calner et al., 2004a). No specific gamma-ray signature can be tied to the Botvide Member. The top of the När Formation is defined by a sharp negative inflexion in the gamma-ray log, marking the boundary with the overlying limestones of the Eke Formation.

The Eke Formation consists of algal limestones, exhibits low gamma-ray values, and encompasses the major rise and peak of the $\delta^{13}C_{carb}$ excursion of the Lau Event (Calner and

Eriksson, 2006a; Younes et al., 2017; Erlström et al., 2022). A sharp increase in gamma-ray values marks the transition to the overlying Burgsvik Formation.

The Burgsvik Formation displays alternating low and high gamma-ray values, reflecting an alternation of siltstones and limestones (Calner and Eriksson, 2006a; Eriksson and Calner, 2008; Erlström et al., 2022). The Burgsvik Formation spans the upper part of the $\delta^{13}C_{carb}$ excursion of the Lau Event (Younes et al., 2017). A decrease in the gamma-ray values marks the boundary to the overlying Hamra/Sundre formations.

Low gamma-ray values mark the Hamra/Sundre formations. The formations coincide with a return to baseline $\delta^{13}C_{carb}$ values (Calner et al., 2004a; Calner and Eriksson, 2006a; Eriksson and Calner, 2008; Erlström et al., 2022). As the youngest units identified, the Hamra and Sundre formations were only encountered in a limited number of wells, limiting the ability to assess internal gamma-ray variability and making correlations less certain.

CONCLUSIONS

This study presents a comprehensive and reproducible workflow that integrates well-log data with DTW/DBA-based algorithms to conduct stratigraphic correlation. The iterative construction of a regional reference curve using the DBA algorithm enabled consistent alignment across multiple well logs, highlighting the potential of DTW-based methods in improving correlations within relatively uniform and synchronous successions.

The workflow was applied to a set of well logs spanning the Silurian succession of central and southern Gotland, enabling a semi-automated correlation that subdivided the subsurface into fifteen distinct geological units. Many of the identified subsurface units were successfully tied to their surface equivalents, though the quality of these correlations varied. Notably, the subdivision of the Hemse Group proved challenging due to significant uncertainties in its internal stratigraphy and boundaries.

The analysis effectively captured gamma-ray log responses associated with key biogeochemical events, including the Ireviken, Mulde, and Lau events, providing valuable

insights into their subsurface expression and confirming their stratigraphic significance. In contrast, the Linde Event could not be identified in the gamma-ray data, emphasizing the need for additional high-resolution $\delta^{13}C_{carb}$ records to refine its stratigraphic placement and improve interpretations of the surrounding units.

REFERENCES

Aldridge, R.J., Jeppsson, L., and Dorning, K.J., 1993, Early Silurian oceanic episodes and events: Journal - Geological Society (London), v. 150, p. 501-513, doi:10.1144/gsjgs.150.3.0501.

Baarli, G.B., Johnson, M.E., and Antoshkina, A.I., 2003, Silurian stratigraphy and paleogeography of Baltica: v. 493, 3-34 p.

Baville, P., Apel, M., Hoth, S., Knaust, D., Antoine, C., Carpentier, C., and Caumon, G., 2022, Computer-assisted stochastic multi-well correlation: Sedimentary facies versus well distality: Marine and Petroleum Geology, v. 135, doi:10.1016/j.marpetgeo.2021.105371.

Biebesheimer, E.J., Cramer, B.D.B.D., Calner, M., Barnett, B.A., Oborny, S.C., and Bancroft, A.M., 2021, Asynchronous δ13Ccarb and δ13Corg records during the onset of the Mulde (Silurian) positive carbon isotope excursion from the Altajme core, Gotland, Sweden: Chemical Geology, v. 576, p. 120256, doi:10.1016/j.chemgeo.2021.120256.

Bjerkéus, M., and Eriksson, M., 2001, Late silurian reef development in the baltic sea: Gff, v. 123, p. 169-179, doi:10.1080/11035890101233169.

Bowman, C.N., Young, S.A., Kaljo, D., Eriksson, M.E., Them, T.R., Hints, O., Martma, T., and Owens, J.D., 2019, Linking the progressive expansion of reducing conditions to a stepwise mass extinction event in the late Silurian oceans: Geology, v. 47, p. 968-972, doi:10.1130/G46571.1.

De Bruin, G., Hemstra, N., and Pouwel, A., 2007, Stratigraphic surfaces in the depositional and chronostratigraphic (Wheeler-transformed) domain: Leading Edge (Tulsa, OK), v. 26, p. 883-886, doi:10.1190/1.2756868.

492 Calner, M., 2005, Silurian carbonate platforms and extinction events - Ecosystem changes
493 exemplified from Gotland, Sweden: Facies, v. 51, p. 584-591, doi:10.1007/s10347-005-
494 0050-0.

495 Calner, M., 2008, Silurian global events - At the tipping point of climate change: Mass
496 Extinction, p. 21-57, doi:10.1007/978-3-540-75916-4_4.

497 Calner, M., 1999, Stratigraphy, facies development, and depositional dynamics of the late
498 wenlock fröjel formation, Gotland, Sweden: Gff, v. 121, p. 13-24,
499 doi:10.1080/11035899901211013.

500 Calner, M., and Eriksson, M.J., 2006a, Evidence for rapid environmental changes in low
501 latitudes during the Late Silurian Lau Event: The Burgen-1 drillcore, Gotland, Sweden:
502 Geological Magazine, v. 143, p. 15-24, doi:10.1017/S001675680500169X.

503 Calner, M., and Eriksson, M.E., 2006b, Silurian research at the crossroads: Gff, v. 128, p.
504 73-74, doi:10.1080/11035890601282073.

505 Calner, M., and Jeppsson, L., 2003, Carbonate platform evolution and conodont stratigraphy
506 during the middle Silurian Mulde Event, Gotland, Sweden: Geological Magazine, v. 140,
507 p. 173-203, doi:10.1017/S0016756802007070.

508 Calner, M., Jeppsson, L., and Munnecke, A., 2004a, The Silurian of Gotland - Part I: Review
509 of the stratigraphic framework, event stratigraphy, and stable carbon and oxygen isotope
510 development: Erlanger geologische Abhandlungen, v. 5, p. 113-131.

511 Calner, M., Kozłowska, A., Masiak, M., and Schmitz, B., 2006, A shoreline to deep basin
512 correlation chart for the middle Silurian coupled extinction-stable isotopic event: Gff, v.
513 128, p. 79-84, doi:10.1080/11035890601282079.

514 Calner, M., Munnecke, A., and Jeppsson, L., 2004b, The Silurian of Gotland - Part II: Guide to
515 the IGCP 503 field meeting 2004: Erlanger geologischen Abhandlungen, v. 5, p. 20.

516 Claussen, A.L., 2024, Benthic response to the strong Silurian climatic uctuations-implications

517 from Gotland (Sweden): Facies, doi:10.1007/s10347-024-00686-x.

518 Cramer, B.D., 2009, Application of Integrated High-Resolution Biochemostratigraphy to
519 Paleozoic Chronostratigraphic Correlation: Recalibrating the Silurian System:,
520 http://rave.ohiolink.edu/etdc/view?acc_num=osu1245178129.

521 Cramer, B.D., Kleffner, M.A., Brett, C.E., McLaughlin, P.I., Jeppsson, L., Munnecke, A., and
522 Samtleben, C., 2010, Paleobiogeography, high-resolution stratigraphy, and the future of
523 Paleozoic biostratigraphy: Fine-scale diachroneity of the Wenlock (Silurian) conodont
524 Kockelella walliseri: Palaeogeography, Palaeoclimatology, Palaeoecology, v. 294, p.
525 232-241, doi:10.1016/j.palaeo.2010.01.002.

526 Dahlqvist, P., and Triumf, C. SkyTEM-undersökningar på Gotland:

527 Edwards, J., Lallier, F., Caumon, G., and Carpentier, C., 2018, Uncertainty management in
528 stratigraphic well correlation and stratigraphic architectures: A training-based method:
529 Computers and Geosciences, v. 111, p. 1-17, doi:10.1016/j.cageo.2017.10.008.

530 Ellis, D. V, and Singer, J.M., 2007, Well Logging for Earth Scientists: v. 53, 1-30 p.,
531 doi:10.1007/978-1-4020-4602-5.

532 Eriksson, M.J., and Calner, M., 2008, A sequence stratigraphical model for the Late Ludfordian
533 (Silurian) of Gotland, Sweden: Implications for timing between changes in sea level,
534 palaeoecology, and the global carbon cycle: Facies, v. 54, p. 253-276,
535 doi:10.1007/s10347-007-0128-y.

536 Erlström, M., and Sopher, D., 2019, Geophysical well log-motifs, lithology, stratigraphical
537 aspects and correlation of the Ordovician succession in the Swedish part of the Baltic
538 Basin: International Journal of Earth Sciences, v. 108, p. 1387-1407, doi:10.1007/s00531-
539 019-01712-y.

540 Erlström, M., Sopher, D., and Dahlqvist, P., 2022, Berggrunden på Sudret, Gotland. Underlag
541 för bedömning av grundvattentillgångar, geoenergipotential samt koldioxidlagring:,
542

www.sgu.se.

Fang, J.H., Chen, H.C., Shultz, A.W., and Mahmoud, W., 1992, Computer-aided well log correlation: American Association of Petroleum Geologists Bulletin, v. 76, p. 307-317, doi:10.1306/bdff87e0-1718-11d7-8645000102c1865d.

Flodén, T., Bjerkéus, M., Tuuling, I., and Eriksson, M., 2001, A silurian reefal succession in the gotland area, baltic sea: Gff, v. 123, p. 137-152, doi:10.1080/11035890101233137.

Frýda, J., Lehnert, O., Joachimski, M.M., Männik, P., Kubajko, M., Mergl, M., Farkaš, J., and Frýdová, B., 2021, The Mid-Ludfordian (late Silurian) Glaciation: A link with global changes in ocean chemistry and ecosystem overturns: Earth-Science Reviews, v. 220, p. 103652, doi:10.1016/j.earscirev.2021.103652.

Giorgino, T., 2009, Computing and visualizing dynamic time warping alignments in R: The dtw package: Journal of Statistical Software, v. 31, p. 1-24, doi:10.18637/jss.v031.i07.

Grant, C.W., Bashore, W.M., and Compton, S., 2018, Rapid Reservoir Modeling with Automated Tops Correlation, *in* Proceedings of the 6th Unconventional Resources Technology Conference, Tulsa, OK, USA, American Association of Petroleum Geologists, doi:10.15530/urtec-2018-2904037.

Hartke, E.R., Cramer, B.D.B.D., Calner, M., Melchin, M.J., Barnett, B.A., Oborny, S.C., and Bancroft, A.M., 2021, Decoupling δ13Ccarb and δ13Corg at the onset of the Ireviken Carbon Isotope Excursion: Δ13C and organic carbon burial (forg) during a Silurian oceanic anoxic event: Global and Planetary Change, v. 196, p. 103373, doi:10.1016/j.gloplacha.2020.103373.

Hay, C.C., Creveling, J.R., Hagen, C.J., Maloof, A.C., and Huybers, P., 2019, A library of early Cambrian chemostratigraphic correlations from a reproducible algorithm: Geology, v. 47, p. 457-460, doi:10.1130/G46019.1.

Hladil, J., Vondra, M., Cejchan, P., Vich, R., Koptikova, L., and Slavik, L., 2010, The dynamic

time-warping approach to comparison of magnetic-susceptibility logs and application to lower devonian calciturbidites (Prague Synform, Bohemian Massif): Geologica Belgica, v. 13, p. 385-406.

Jeppsson, L., 1987, Lithological and conodont distributional evidence for episodes of anomalous oceanic conditions during the Silurian, *in* Palaeobiology of conodonts., p. 12-145.

Jeppsson, L., 1996, Recognition of a probable secundo-primo event in the Early Silurian: Lethaia, v. 29, p. 311-315, doi:10.1111/j.1502-3931.1996.tb01666.x.

Jeppsson, L., 1998, Silurian oceanic events. Summary of general characteristics, *in* New York State Museum Bulletin, p. 239-257.

Jeppsson, L., and Aldridge, R.J., 2000, Ludlow (late Silurian) oceanic episodes and events: Journal of the Geological Society, v. 157, p. 1137-1148, doi:10.1144/jgs.157.6.1137.

Jeppsson, L., Aldridge, R.J., and Dorning, K.J., 1995, Wenlock (Silurian) oceanic episodes and events: Journal - Geological Society (London), v. 152, p. 487-498, doi:10.1144/gsjgs.152.3.0487.

Jeppsson, L., and Calner, M., 2002, The silurian mulde event and a scenario for secundo-secundo events: Transactions of the Royal Society of Edinburgh, Earth Sciences, v. 93, p. 135-154, doi:10.1017/S0263593300000377.

Jeppsson, L., Eriksson, M.E., and Calner, M., 2006, A latest Llandovery to latest Ludlow high-resolution biostratigraphy based on the Silurian of Gotland - a summary: Gff, v. 128, p. 109-114, doi:10.1080/11035890601282109.

Jorgensen, F. et al., 2018, A 3D geological model of the Island of Gotland based on extensive airborne EM mapping , seismic data and log stratigraphy A 3D geological model of the Island of Gotland based on extensive airborne EM mapping , seismic data and log stratigraphy .: EAM2018 7th International Workshop on Airborne Electromagnetics, p.

1-4.

Lallier, F., Caumon, G., Borgomano, J., Viseur, S., Fournier, F., Antoine, C., and Gentilhomme, T., 2012, Relevance of the stochastic stratigraphic well correlation approach for the study of complex carbonate settings: Application to the Malampaya buildup (Offshore Palawan, Philippines): Geological Society Special Publication, v. 370, p. 265-275, doi:10.1144/SP370.12.

Lallier, F., Caumon, G., Borgomano, J., Viseur, S., Royer, J.J., and Antoine, C., 2016, Uncertainty assessment in the stratigraphic well correlation of a carbonate ramp: Method and application to the Beausset Basin, SE France: Comptes Rendus - Geoscience, v. 348, p. 499-509, doi:10.1016/j.crte.2015.10.002.

Lazauskiene, J., Sliaupa, S., Brazauskas, A., and Musteikis, P., 2003, Sequence stratigraphy of the Baltic Silurian succession: Tectonic control on the foreland infill: Geological Society Special Publication, v. 208, p. 95-115, doi:10.1144/GSL.SP.2003.208.01.05.

Levendal, T., Sopher, D., Juhlin, C., and Lehnert, O., 2019, Investigation of an Ordovician carbonate mound beneath Gotland, Sweden, using 3D seismic and well data: Journal of Applied Geophysics, v. 162, p. 22-34, doi:10.1016/j.jappgeo.2019.01.008.

Lineman, D., Mendelson, J., and Toksoz, M., 1987, Well to well log correlation using knowledgebased systems and dynamic depth warping: Transactions of SPWLA 28th Annual Logging Symposium, p. 1-25.

Lomask, J., Francis, J.M., Rickett, J., Buursink, M.L., Gerber, T.P., Perlmutter, M., and Paola, C., 2009, New tools for seismic stratigraphie interpretation: Strata! convergence and instantaneous isochron attribute cubes derived from volumetric flattening of experimental strata: AAPG Bulletin, v. 93, p. 453-459, doi:10.1306/11200808104.

Männik, P., Loydell, D.K., Nestor, V., and Nõlvak, J., 2015, Integrated Upper Ordovician-lower Silurian biostratigraphy of the Grötlingbo-1 core section, Sweden: Gff, v. 137, p. 226-244, doi:10.1080/11035897.2015.1042032.

619 Manten, A.A., 1971, Silurian Reefs of Gotland: Developments in Sedimentology, p. 539,
620 doi:10.1017/S0016756800056922.

621 McLaughlin, P.I., Emsbo, P., Brett, C.E., Bancroft, A.M., Desrochers, A., and Vandenbroucke,
622 T.R.A., 2019, The rise of pinnacle reefs: A step change in marine evolution triggered by
623 perturbation of the global carbon cycle: Earth and Planetary Science Letters, v. 515, p.
624 13-25, doi:10.1016/j.epsl.2019.02.039.

625 Melchin, M.J., Sadler, P.M., and Cramer, B.D., 2020, Chapter 21 - The Silurian Period, *in*
626 Gradstein, F.M., Ogg, J.G., Schmitz, M.D., and Ogg, G.M. eds., Geologic Time Scale
627 2020, Elsevier, p. 695-732, doi:https://doi.org/10.1016/B978-0-12-824360-2.00021-8.

628 Melchin, M.J., Sadler, P.M., Cramer, B.D., Cooper, R.A., Gradstein, F.M., and Hammer, Ø.,
629 2005, The silurian period (F. M. Gradstein, J. G. Ogg, M. D. Schmitz, & G. M. Ogg, Eds.):
630 Elsevier, 188-201 p., doi:10.1016/B978-0-444-59425-9.00021-4.

631 Meyers, S.R., 2019, Cyclostratigraphy and the problem of astrochronologic testing: Earth-
632 Science Reviews, v. 190, p. 190-223, doi:10.1016/j.earscirev.2018.11.015.

633 Nieminski, N.M., Sylvester, Z., Covault, J.A., Gomberg, J., Staisch, L., and McBrearty, I.W.,
634 2024, Turbidite correlation for paleoseismology: Geological Society of America Bulletin,
635 p. 1-12, doi:10.1130/b37343.1.

636 Petitjean, F., Ketterlin, A., and Gançarski, P., 2011, A global averaging method for dynamic
637 time warping, with applications to clustering: Pattern Recognition, v. 44, p. 678-693,
638 doi:10.1016/j.patcog.2010.09.013.

639 Qayyum, F., Catuneanu, O., and de Groot, P., 2015, Historical developments in Wheeler
640 diagrams and future directions: Basin Research, v. 27, p. 336-350,
641 doi:10.1111/bre.12077.

642 Radzevičius, S., Spiridonov, A., and Brazauskas, A., 2014, Integrated middle-upper Homerian
643 (Silurian) stratigraphy of the Viduklė-61 well, Lithuania: Gff, v. 136, p. 218-222,
644

doi:10.1080/11035897.2013.866976.

Rose, C. V., Fischer, W.W., Finnegan, S., and Fike, D.A., 2019, Records of carbon and sulfur cycling during the Silurian Ireviken Event in Gotland, Sweden: Geochimica et Cosmochimica Acta, v. 246, p. 299-316, doi:10.1016/j.gca.2018.11.030.

Samtleben, C., Munnecke, A., and Bickert, T., 2000, Development of facies and C/O-isotopes in transects through the Ludlow of Gotland: Evidence for global and local influences on a shallow-marine environment: Facies, v. 43, p. 1-38, doi:10.1007/bf02536983.

Samtleben, C., Munnecke, A., Bickert, T., and Pätzold, J., 1996, The Silurian of Gotland (Sweden): Facies interpretation based on stable isotopes in brachiopod shells: Geologische Rundschau, v. 85, p. 278-292, doi:10.1007/BF02422234.

Sardá-Espinosa, A., 2019, Time-series clustering in R Using the dtwclust package: R Journal, v. 11, p. 1-45, doi:10.32614/rj-2019-023.

Sopher, D., Erlström, M., Bell, N., and Juhlin, C., 2016, The structure and stratigraphy of the sedimentary succession in the Swedish sector of the Baltic Basin: New insights from vintage 2D marine seismic data: Tectonophysics, v. 676, p. 90-111, doi:10.1016/j.tecto.2016.03.012.

Stolfus, B.M., Allman, L.J., Young, S.A., Calner, M., Hartke, E.R., Oborny, S.C., Bancroft, A.M., and Cramer, B.D., 2023, Expansion of Reducing Marine Environments During the Ireviken Biogeochemical Event: Evidence From the Altajme Core, Gotland, Sweden: Paleoceanography and Paleoclimatology, v. 38, doi:10.1029/2022PA004484.

Sylvester, Z., 2023, Automated multi-well stratigraphic correlation and model building using relative geologic time: Basin Research, v. 35, p. 1961-1984, doi:10.1111/bre.12787.

Tuuling, I., and Flodén, T., 2013, Silurian reefs off Saaremaa and their extension towards Gotland, central Baltic Sea: Geological Magazine, v. 150, p. 923-936, doi:10.1017/S0016756813000101.

Tuuling, I., and Flodén, T., 2009, The Llandovery-lowermost Wenlock sequence in the Baltic Sea between Saaremaa and Gotland; subdivision, thicknesses and correlation, based on marine seismic studies: Marine Geology, v. 267, p. 55-70, doi:10.1016/j.margeo.2009.09.004.

Vandenbroucke, T.R.A., Munnecke, A., Leng, M.J., Bickert, T., Hints, O., Gelsthorpe, D., Maier, G., and Servais, T., 2013, Reconstructing the environmental conditions around the Silurian Ireviken Event using the carbon isotope composition of bulk and palynomorph organic matter: Geochemistry, Geophysics, Geosystems, v. 14, p. 86-101, doi:10.1029/2012GC004348.

Wheeler, L., and Hale, D., 2014, Simultaneous correlation of multiple well logs: Society of Exploration Geophysicists International Exposition and 84th Annual Meeting SEG 2014, p. 618-622, doi:10.1190/segam2014-0227.1.

Wu, X., Li, Y., and Sawasdee, P., 2022, Toward accurate seismic flattening: Methods and applications: GEOPHYSICS, v. 87, p. IM177-IM188, doi:10.1190/geo2021-0662.1.

Wu, X., Shi, Y., Fomel, S., and Li, F., 2018, Incremental correlation of multiple well logs following geologically optimal neighbors: Interpretation, v. 6, p. T713-T722, doi:10.1190/INT-2018-0020.1.

Younes, H., Calner, M., and Lehnert, O., 2017, The first continuous δ13C record across the Late Silurian Lau Event on Gotland, Sweden: Gff, v. 139, p. 63-69, doi:10.1080/11035897.2016.1227362.

Zoraster, S., Paruchuri, R., and Darby, S., 2004, Curve Alignment for Well-to-Well Log Correlation, *in* SPE Annual Technical Conference and Exhibition, SPE, doi:10.2118/90471-MS.

ACKNOWLEDGMENTS

The FNRS-PDR T.0051.19 grant financially supported Michiel Arts. Anne-Christine Da Silva acknowledges the “Conseil Universitaire de la recherche et la valorisation,”. Rohit Samant has been funded by the Deutsche Forschungsgemeinschaft (VL96/9-1, grant no. 527307807).

Supplementary Information

The dataset used to produce the results in this study, along with the R code, is available.: DOI: 10.5281/zenodo.17342729, https://zenodo.org/records/17342729

SI.1. Well-log origins

			Source: some logs have been digitized multiple times, and as such have multiple sources				
well name	X	Y	SGU OPAB digitized. LAS file	OPAB digitized by Michiel Arts	Leventhal 2019	SGU digital logs	remark
Altajme	1662465	6365981				x	
Bofride-1	1670487	6360752	x				
Dalsviden-1	1660944	6344417	x	x			
Djaupdy-1	1675458	6350616	x	x			
Faludden-2	1655703	6322416		x			
Gervalds-1	1644364	6316651		x			
Gläves-1	1665362	6349113	x	x			
Grötlingbo-1	1660000	6335550	x				Not a Gr log
Grötlingbo-2	1660138	6335746	x				Not a Gr log
Hammaren-1	1674764	6352755		x			
Hemse-1	1656198	6349003	x	x			
Kastelle-1	1646554	6321248	x	x			
Kauparve-1	1657906	6335536	x	x			
Klasen-1	1659273	6335899	x	x			
Kvarne-1	1645813	6319704		x			
Kvarne-2	1646331	6319877	x	x			
Lau-1	1670030	6354383	x	x			
Linhatte-1	1652237	6317891	x	x			
Lukse-2	1663320	6345563			x		
Maldes-1	1671193	6350654	x		x		
Mattise-1	1669769	6350160	x	x			
Nyudden-1	1675330	6352841	x	x			
Nyudden-2	1673659	6352678		x			
Östergarn-1	1685649	6370272	x	x			
Ostris-1	1657840	6343430	x	x			
Pete-1	1643596	6338729			x		
Rojrviken-1	1651662	6320212	x	x			
Ronehamn-1	1661911	6341637	x	x			
Sigdes-1	1664442	6350284	x	x			
Silte-1	1647050	6346654	x	x			
Sindarve-1	1654208	6319914	x	x			
Skåls-1	1645247	6329560	x	x			
Skärsbod-1	1649541	6332097	x	x			
Storms-1	1648178	6319293	x	x			
St.Sutarve-2018	1651134	6320497				x	
Sundre-1-A	1644533	6314706	x	x			

Sundre-1-B	1644533	6314706		x			
Vannes-1	1646136	6315815	x	x			
Vastergarde-1	1652152	6328478	x	x			
Vike-1	1682657	6372151	x		x		

SI.2. Tracking the well log motif of the Mulde Event

The Grötlingbo-1 contains the Mulde Event at ~250 m depth (Calner et al., 2006). The density log of the Grötlingbo-1 wells shows a large anomaly between 255 and 247 m. This anomaly can also be observed in the resistivity log of the Grötlingbo-2 as well (located ~40 m southwest of the Grötlingbo-1 log). The same anomaly in the well-logs can be tracked and observed in the nearby Kauparve-1 well, which has both resistivity and gamma-ray data available. This allows us to correlate the Mulde Event with the gamma-ray log. These identified boundaries are in agreement with other records in the basin, where both the $\delta^{13}C_{carb}$ excursion of the Mulde Event and a gamma-ray curve are available (Radzevičius et al., 2014b, 2014a, 2017).

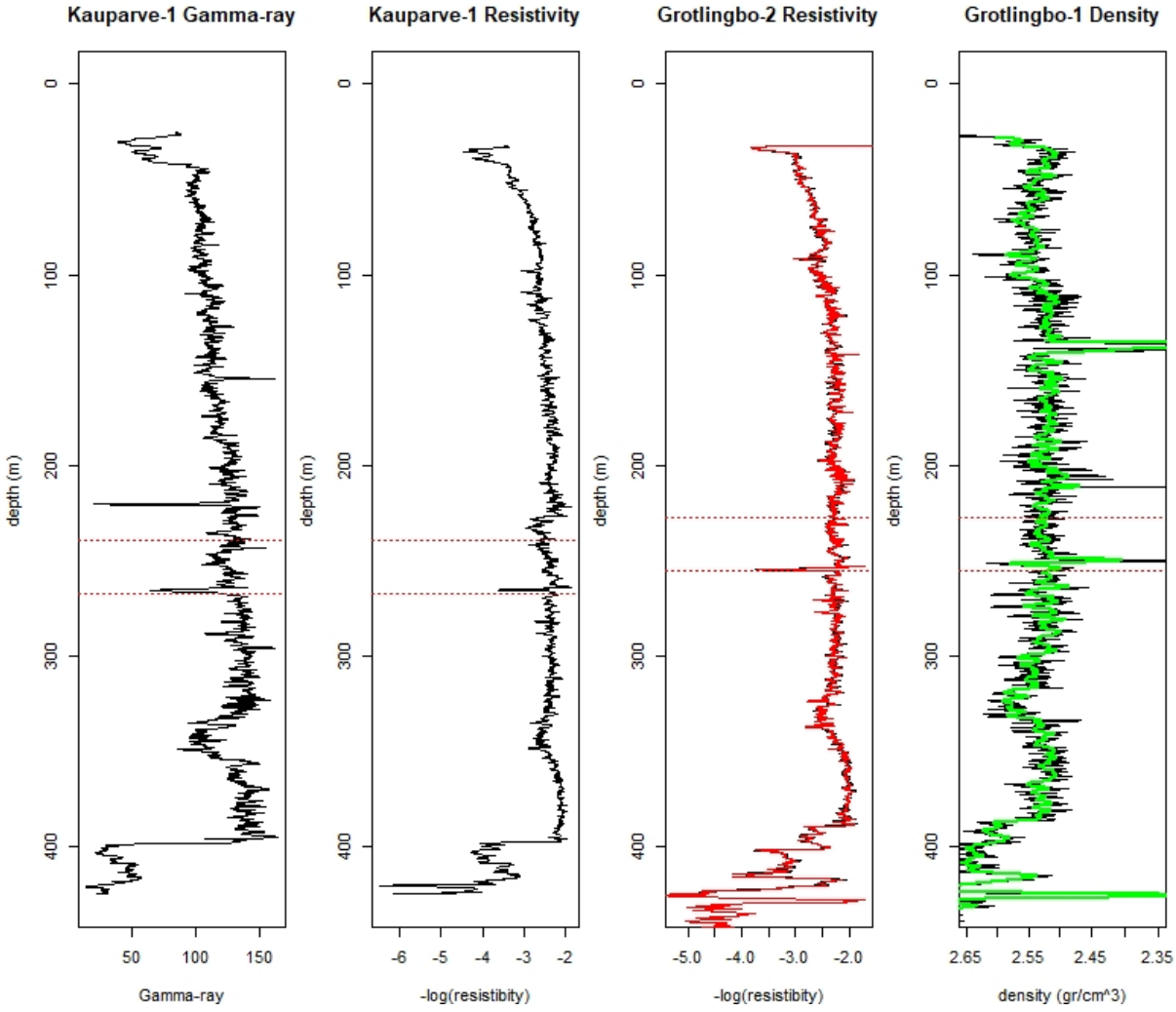

SI. Figure 1. Well-logs of the Kauparve-1, Grötlingbo-2, and Grötlingbo-1 wells. The red horizontal dotted lines mark the start and end of the Mulde Event. The black line in the Grötlingbo-2 well is the digitised resistivity well log (plotted on an inverted log scale), as performed as part of this study. The red line in the Grötlingbo-2 well is a digitised well log as performed at SGU (plotted on an inverted log scale). The green line in the Grötlingbo-1 well is the smoothed density curve using a window of 2 meters.

SI.3. R code

See SI_3_well_logs_gotland_github.R

Si.4. Dataset

See the SI_4_GR_logs_used folder.